

Broadening the optical bandwidth of quantum cascade lasers using RF noise current perturbations

TOMÁS H. P. PINTO¹, JAMES M. R. KIRKBRIDE¹, AND GRANT A. D. RITCHIE^{1,*}

¹Department of Chemistry, The Physical and Theoretical Chemistry Laboratory, The University of Oxford, South Parks Road, OX1 3QZ, United Kingdom

*Corresponding author: grant.ritchie@chem.ox.ac.uk

Compiled April 18, 2018

We report on the broadening of the optical bandwidth of a distributed feedback quantum cascade laser (QCL) caused by the application of radio frequency (RF) noise to the injection current. The broadening is quantified both via Lamb-dip spectroscopy and the frequency noise power spectral density (PSD). The linewidth of the unperturbed QCL (emitting at $\sim 5.3 \mu\text{m}$) determined by Lamb-dip spectroscopy is $680 \pm 170 \text{ kHz}$, and is in reasonable agreement with the linewidth of $460 \pm 40 \text{ kHz}$ estimated by integrating the PSD measured under the same laser operating conditions. Measurements with both techniques reveal that by mixing the driving current with broadband RF noise the laser lineshape was reproducibly broadened up to *ca* 6 MHz with an increasing Gaussian contribution. The effects of linewidth broadening are then demonstrated in the two colour coherent transient spectra of nitric oxide. ©

2018 Optical Society of America

OCIS codes: (300.6460) Spectroscopy, saturation; (300.3700) Linewidth; (300.6240) Spectroscopy, coherent transient.

<http://dx.doi.org/10.1364/ao.XX.XXXXXX>

Quantum cascade lasers (QCLs) as mid-infrared sources have gained popularity in the last two decades finding applications in areas such as high resolution spectroscopy, non-linear optics and trace gas sensing.[1–3] This is due to their high optical emission power (usually in the hundreds of mW), narrow linewidths (typically a few MHz or less), and near room-temperature operation.[4] High resolution spectroscopic techniques such as saturation spectroscopy benefit from these narrow linewidths, and are tools for establishing accurate frequency markers and laser stabilization[5, 6]. The high coherence and intensity of the electric field produced by these sources also allows the observation of coherent transient effects when the laser frequency is swept over a strong molecular transition of a velocity selected sample on a timescale that is short compared to its relaxation time.[7–9] These non-linear optical effects, which include Rabi cycling and optical nutation, are highly dependent on the linewidth of the laser that prepares the velocity selected sample. The excitation of a wider range of velocity groups suppresses coherent effects, as will be shown later in this work.

For trace gas sensing, high fidelity QCLs have been imple-

mented in a range of optical cavity techniques such as off-axis cavity enhanced absorption spectroscopy (OA-CEAS), cavity ring-down spectroscopy (CRDS) and optical-feedback cavity enhanced absorption spectroscopy (OF-CEAS). [10–15] While resonant cavity techniques like OF-CEAS provide the highest sensitivities in general, OA-CEAS retains attractive features relating to practicality, including robustness, ease of alignment, frequency resolution and compactness.[16] These are a consequence of a *modus operandi* for OA-CEAS which requires a dense, random mode structure from which to generate a smooth time-integrated cavity transmission spectrum as the laser frequency is scanned. Such attributes are particularly pertinent for example, in the construction of in-line breath sensors where rapidly varying flows occur.[17] A drawback of OA-CEAS is that it is a low signal technique (because the cavity is non-resonant) and therefore the high powers of cw QCLs are beneficial. In such instruments the intensity noise arising from the residual mode structure is often the sensitivity limiting factor and is most apparent with narrow linewidth lasers. Strategies to reduce the residual mode noise in these non-resonant techniques have included dithering the laser frequency or the cavity length; the latter usually achieved using a piezo-electric transducer.[18] An alternative method for improving the sensitivity of OA-CEAS was demonstrated by Ciaffoni *et al*, who showed that the introduction of random frequency fluctuations induced by mixing broadband radio-frequency (RF) noise with the driving current of a VCSEL operating at 764 nm resulted in residual mode noise suppression.[19] Similarly, Manfred *et al* have shown that the sensitivity of a QCL based OA-CEAS spectrometer was enhanced by nearly an order of magnitude by employing the same current perturbation scheme.[20] The residual mode noise suppression resulting from perturbation of the injection current is due to laser linewidth broadening, making it clear that tuned linewidth sources are advantageous in a laser spectrometer of this type. While this enhancement has been predicted theoretically[21], the actual impact of broadband RF perturbations on QCL linewidth requires further investigation.

The linewidth of QCLs has been experimentally determined in several ways, including two-sample (Allan) variance[22], by analysing the noise power spectral density (PSD) of optical emission[23, 24] (using the side of a molecular transition as a frequency discriminator) and by Lamb-dip spectroscopy[9, 25]. In this work, the linewidth of a QCL operating at $\sim 5.3 \mu\text{m}$ is measured via Lamb-dip spectroscopy on a low pressure sam-

ple of NO and by analysing the frequency noise power spectral density of the system using a Ge etalon as a frequency discriminator. The impact of RF noise perturbations on the linewidth of a QCL is quantified, and the ability to control the extent of the line broadening by amplifying the noise by different factors is demonstrated.

The experimental procedures are conducted on a single mode cw distributed feedback (DFB) QCL (Maxion M575AH-NS), which emits over the range 1897-1904 cm^{-1} with output powers up to 250 mW, cooled by a two stage peltier thermo-electric cooler (TEC) and driven by a custom designed driver. The driving current is mixed with broadband (50 kHz to 500 MHz) RF noise (RFDesignUK, Noise Brick - NB 3) via a bias tee, and is amplified up to +25 dB (Mini-circuits MHF model).

For Lamb-dip spectroscopy, a CaF_2 window is used to split the laser beam into a strong pump beam and a weak probe beam containing about 95% and 5% of the laser output power, respectively. The two beams counter propagate through a 73 cm long cell with a crossing angle of 0.2° . The laser frequency is scanned by applying a triangular voltage ramp to the driver by the means of a function generator (TTi TG230). The probe beam is detected by a photodiode (VIGO PVMI-3TE-10.6). An outline of this experimental setup can be found in work published by Kirkbride *et al*[9]. The DFB QCL probes the $R(6.5)_{\frac{1}{2}} v = 1 \leftarrow 0$ transition of the electronic ground state of NO at 1900.07 cm^{-1} and at a total gas pressure of 50 mTorr.

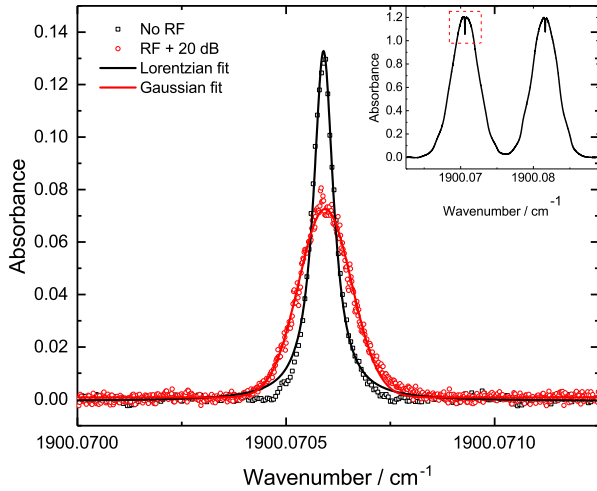


Fig. 1. Lamb dips with Lorentzian and Gaussian fits for the cases of unperturbed injection current and with the application of RF noise (+20 dB) respectively. The inset shows the full range of the frequency scan before the subtraction of the Doppler profiles. The low frequency noise present at the sides of the profiles is caused by residual optical feedback due to the spatial proximity of the counter-propagating pump and probe beams, and is absent if either of the beams is blocked.

The inset of Figure 1 shows the Doppler profiles associated with the $R(6.5)_{\frac{1}{2}}$ transition. This rovibrational transition presents a doublet structure since NO has a $^2\Pi$ electronic ground state and is subject to Λ -doubling. In addition, hyperfine coupling with the nuclear spin of nitrogen ($I = 1$) will be responsible for further splitting of each Λ component into six hyperfine components, from which only the three strongest are observable and saturable with the laser intensity available. The hyperfine

interaction is weak, so the splitting between the most widely separated hyperfine components is only 540 kHz for the e Λ -component and 1.26 MHz for the f Λ -component, resulting in a single dip in both cases.

The Doppler profiles are subtracted from the spectrum and the Lamb dip of the e component is shown in the main part of Figure 1 along with fits to the data obtained with and without RF perturbation of the laser injection current. For the unperturbed case the data are fit with the sum of three Lorentzian functions. These functions are of equal width and centered at the position of each hyperfine component, which yield a FWHM of 1.56 ± 0.17 MHz. The spectra are averaged 100 times, and the error is obtained from the standard deviation of the width of all individual sweeps. The measured FWHM includes contributions from collisional broadening, which is 240 kHz at 50 mTorr of NO (with $\gamma_{\text{self}} = 4.9 \text{ MHz Torr}^{-1}$ [26]), transit-time broadening of ~ 320 kHz with a beam radius of 1 mm, and residual Doppler broadening of 320 kHz. Removing these contributions yields a linewidth of 680 ± 170 kHz. At a chirp rate of $0.15 \text{ MHz } \mu\text{s}^{-1}$, the time taken to traverse the dip (FWHM of 1.73 MHz) is $11.5 \mu\text{s}$; this establishes a lower limit for the observation time. As seen in Figure 1, by perturbing the injection current with the RF noise device coupled to a +20 dB gain amplifier, the linewidth increases to 3.67 ± 0.23 MHz. The evolution of the width as a function of noise is provided further on in this work (see Figure 4). Notably, while the lineshape without RF noise should have both Gaussian and Lorentzian contributions owing to the laser being affected by both white and $1/f$ noise, and thus be described by a Voigt profile, it is found that a Lorentzian function returns a better fit to the unperturbed lineshape. As broadband RF noise is added to the injection current, the Lamb-dip profile becomes progressively more Gaussian; this is expected since the added noise is white, bandwidth limited and hence not statistically correlated.[19]

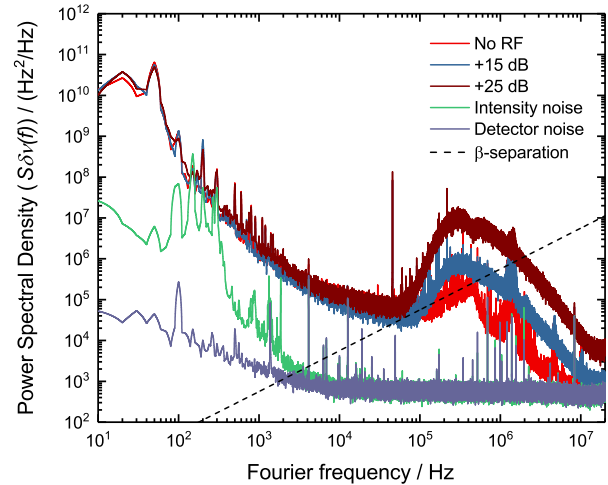


Fig. 2. Noise power spectral density (PSD), $S_{\delta v}(f)$, measured for a range of RF perturbation gains, along with the detector and intensity noise levels. The β -separation line separates the high and low frequency regimes at the point of intersection with the PSD.

The impact of introducing RF perturbations to the injection current is also investigated through acquiring the noise PSD of the system, $S_{\delta v}(f)$, where δv represents the laser frequency deviation around its centre value. In order to do this, an opti-

cal frequency discriminator is necessary to convert frequency fluctuations into amplitude fluctuations. This is achieved by centring the laser frequency on the side of a transmission fringe of a low finesse Ge etalon (493 MHz free spectral range), while keeping the same laser operating conditions as in the Lamb dip measurements. After passing through the etalon, the laser beam is collected onto a 20 MHz bandwidth photodiode (VIGO PVMI-3TE-10.6) and recorded using an oscilloscope (LeCroy Wavesurfer 400 MHz). The PSD is generated using a standard MATLAB Fourier transform routine and the slope of the etalon fringe to obtain an amplitude to frequency conversion factor; in this case, a conversion factor of $163.9 \pm 8.5 \text{ MHz V}^{-1}$ is used.

Figure 2 shows how the optical PSD of the unperturbed laser is modified by RF current perturbations, producing an increase in frequency noise up to a factor of 100 centered at 300 kHz. The intensity noise is obtained by repeating the measurement procedure without a frequency discriminator, while the detector noise is obtained simply by blocking the laser beam. The resulting PSD spectra provide the information necessary for constructing the laser lineshape by employing the theory developed by Di Domenico *et al*[23]. The PSD can be split into two regions that contribute either to the linewidth or the wings of the spectrum. This separation is defined by the line represented in Figure 2, known as the β -separation line, given by $8 \ln 2f / \pi^2$, where f is the Fourier frequency. The region that contributes to the linewidth, defined by $S_{\delta\nu}(f) > 8 \ln 2f / \pi^2$, is a region of high modulation index β . Conversely, the region where $S_{\delta\nu}(f) < 8 \ln 2f / \pi^2$ is a low modulation index region and only contributes to the wings of the lineshape and not the linewidth. The PSD can be used to compute the autocorrelation function and, according to the Wiener-Khinchine theorem, can then be Fourier transformed to produce the lineshapes[23]. The results of this procedure are presented in Figure 3. The integration was performed employing a low frequency cutoff of 200 Hz, which corresponds to an observation time of 5 ms, in order to be consistent with the exclusion of flicker noise.[24]

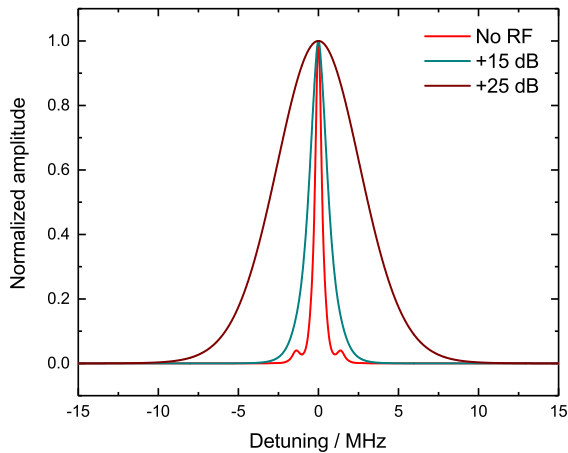


Fig. 3. Laser lineshapes simulated via the frequency noise power spectral density.

In the unperturbed case, the calculated laser lineshape has a FWHM of $460 \pm 40 \text{ kHz}$, which is in reasonable agreement with the width extracted from the Lamb-dip. The two sidebands separated by *ca* 1.5 MHz from the central line could be a result from the frequency noise following the β -separation line between 100 kHz and 400 kHz. The lineshape is best fit by a Lorentzian

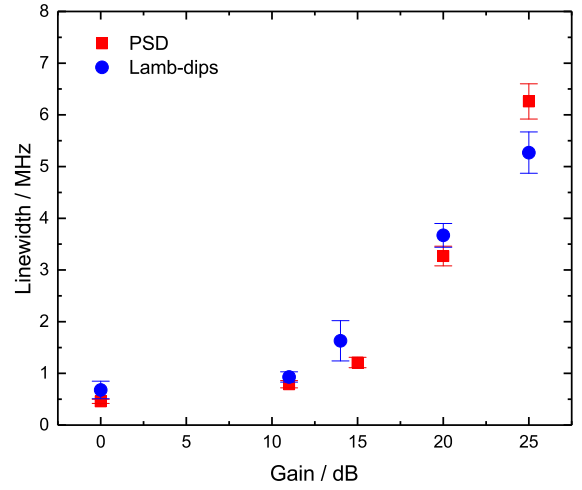


Fig. 4. Laser linewidths for unperturbed and perturbed injection currents as measured by the two distinct techniques.

function with a smaller Gaussian contribution, similarly to the Lamb-dip observations, but quickly evolves to become more Gaussian like once the injection current is perturbed by RF noise. The evolution of the linewidth as a function of RF gain level is presented in Figure 4, showing a steady linewidth increase up to $6.26 \pm 0.34 \text{ MHz}$ at +25 dB gain.

As previously mentioned, the linewidth measured via Lamb-dip spectroscopy has a lower limit of observation time of 11.5 μs . To simulate the lineshape at the same observation time using the frequency noise, a low frequency cutoff of *ca* 100 kHz would have to be implemented. In the unperturbed case, imposing such a limit causes problems due to its close proximity to the low modulation index region. However, as RF noise is added, higher frequencies will enter the high modulation index region as they move above the β -separation line, allowing the 100 kHz cutoff to be implemented in data above +15 dB gain. A comparison between the linewidth with a 200 Hz or a 100 kHz cutoff at > +15 dB revealed only a negligible change in the FWHM. Such comparison is not possible in the unperturbed case for the reason mentioned above. However, using the approximation[23, 24]

$$\text{FWHM} = \sqrt{8 \ln 2 A} \quad (1)$$

where A is the geometric area under the high modulation index region, an approximate linewidth in the unperturbed case can be obtained by integrating the frequency noise using a low frequency cutoff of 100 kHz; a linewidth of $\sim 500 \text{ kHz}$ is thus obtained. This is in good agreement with both the linewidth of $460 \pm 60 \text{ kHz}$ acquired through the Fourier transform method using a 200 Hz cutoff, as well as with the Lamb-dip observations. From this, it can be concluded that the linewidth of the QCL with a 5 ms observation time is nearly identical to that with a 11.5 μs observation time, since the frequency noise drops below $10^6 \text{ (Hz}^2/\text{Hz)}$ at 1 kHz Fourier frequency, corresponding to an observation time of 1 ms. Using the PSD over Lamb-dip spectroscopy for measuring laser linewidths has the clear advantage of allowing the computation of the linewidth at different observation times by adjusting the low frequency cutoff of integration, while only requiring a single measurement. However, both techniques reveal that the QCL linewidth can be reliably tuned within the range of a few MHz by simply adjusting the level of RF current perturbation.

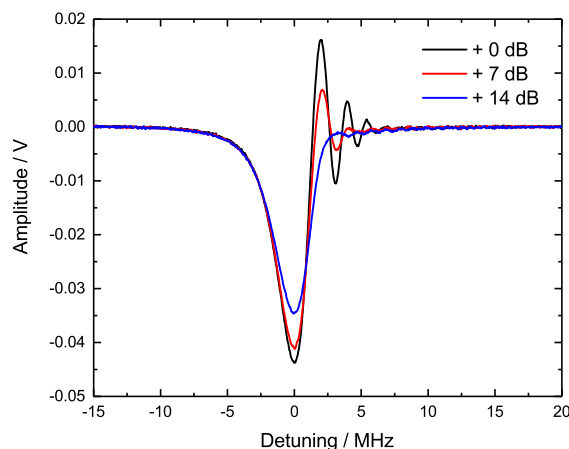


Fig. 5. Rapid passage signals observed in a 2 colour pump and probe experiment on NO with and without RF perturbations at different gain levels, highlighting the high susceptibility of the oscillations to the linewidth of the pump laser.

In order to test the effect of linewidth broadening for studies of non-linear optics, a 2 laser cw pump and probe experiment was conducted on a sample of pure NO at a total pressure of 4 mTorr. Rapid passage coherent transient signals are measured as the tunable linewidth laser pumps the $\text{NO } ^2\Pi_{1/2} \text{ R}(6.5)_{\frac{1}{2}} v = 1 \leftarrow 0$ transition and the second laser probes the velocity selected sample by rapidly sweeping ($7.8 \text{ MHz } \mu\text{s}^{-1}$) over the $^2\Pi_{1/2} \text{ P}(7.5) v = 2 \leftarrow 1$ transition. The signals produced are presented in Figure 5. As the probe laser sweeps over the velocity selected sample in under $1 \mu\text{s}$, a net polarization of molecular dipoles is generated and interacts with the electric field of the chirping laser. Such interaction results in interference which produces the oscillations after the laser is detuned from resonance with the molecular transition. These are rapid passage oscillations, and a key factor that determines their decay time is the width of the velocity selected sample. It becomes clear from Figure 5 that as the RF perturbation gain increases and the pump linewidth varies from *ca* 500 kHz to *ca* 1.3 MHz, a significant decrease in coherence is observed; the rapid passage oscillations are dampened due to velocity dephasing.

In conclusion, the linewidth of a DFB-QCL can be reproducibly modified by perturbing the injection current with RF noise. The extent of broadening has been quantified through saturation spectroscopy and by characterising the frequency noise of the system. A drawback of using Lamb dip spectroscopy is that in order to measure the laser linewidth at a different observation time, the laser chirp rate has to be changed and a new set of experiments is needed, while a single noise PSD measurement is enough for simulating the lineshape at a variety of observation times simply by changing the low frequency cutoff. A practical example of linewidth broadening is demonstrated by the loss of coherence due to velocity dephasing of rapid passage signals, when an increase in linewidth by nearly a factor of 3 almost completely dephases the oscillations. The ability to tune the laser linewidth should also find ready applications in optimizing trace gas sensors based upon OA-CEAS.

Funding. This work was funded by the Natural Environment Research Council (NERC) (NE/M016439/1) and (NE/K008250/1).

REFERENCES

1. C. Gmachl, F. Capasso, D. Sivco, and A. Cho, *Rep. on Prog. Phys.* **64**, 1533 (2001).
2. G. Duxbury, N. Langford, M. T. McCulloch, and S. Wright, *Chem. Soc. Rev.* **34**, 921 (2005).
3. G. Wysocki, R. Lewicki, R. F. Curl, F. K. Tittel, L. Diehl, F. Capasso, M. Troccoli, G. Hoffer, D. Bour, S. Corzine, R. Maulini, M. Giovannini, and J. Faist, *Appl. Phys. B: Lasers Opt.* **92**, 305 (2008).
4. R. F. Curl, F. Capasso, C. Gmachl, A. A. Kosterev, B. McManus, R. Lewicki, M. Pusharsky, G. Wysocki, and F. K. Tittel, *Chem. Phys. Lett.* **487**, 1 (2010).
5. J. Remillard, D. Uy, W. Weber, F. Capasso, C. Gmachl, A. Hutchinson, D. Sivco, J. Baillargeon, and A. Cho, *Opt. Express* **7**, 243 (2000).
6. S. Borri, S. Bartalini, I. Galli, P. Cancio, G. Giusfredi, D. Mazzotti, A. Castrillo, L. Gianfrani, and P. De Natale, *Opt. Express* **16**, 11637 (2008).
7. M. T. McCulloch, G. Duxbury, and N. Langford, *Mol. Phys.* **104**, 2767 (2006).
8. G. Duxbury, J. F. Kelly, T. A. Blake, and N. Langford, *J. Chem. Phys.* **136** (2012).
9. J. M. R. Kirkbride, S. K. Causier, E. A. McCormack, D. Weidmann, and G. A. D. Ritchie, *Phys. Chem. Chem. Physics: PCCP* **15**, 2684 (2013).
10. A. O'Keefe, J. J. Scherer, and J. B. Paul, *Chem. Phys. Lett.* **307**, 343 (1999).
11. X. Lou, Y. Dong, D. Wu, J. Wei, and Z. Lu, *Appl. Phys. B: Lasers Opt.* **121**, 171 (2015).
12. T. P. J. Blaikie, J. Couper, G. Hancock, P. L. Hurst, R. Peverall, G. Richmond, G. A. D. Ritchie, D. Taylor, and K. Valentine, *Anal. Chem.* **88**, 11016 (2016).
13. K. M. Manfred, L. Ciaffoni, and G. A. D. Ritchie, *Appl. Phys. B-Lasers Opt.* **120**, 329 (2015).
14. A. De, G. D. Banik, A. Maity, M. Pal, and M. Pradhan, *Opt. Lett.* **41**, 1949 (2016).
15. I. Ventrillard, P. Gorrotxategi-Carbajo, and D. Romanini, *Appl. Phys. B: Lasers Opt.* **123**, 1 (2017).
16. A. O'Keefe, *Chem. Phys. Lett.* **293**, 331 (1998).
17. C. Wang and P. Sahay, *Sensors* **9**, 8230 (2009).
18. X. Liu, Y. Xu, Z. Su, W. S. Tam, and I. Leonov, *Appl. Phys. B: Lasers Opt.* **102**, 629 (2011).
19. L. Ciaffoni, J. Couper, G. Hancock, R. Peverall, P. A. Robbins, and G. A. D. Ritchie, *Opt. Express* **22**, 17030 (2014).
20. K. M. Manfred, J. M. R. Kirkbride, L. Ciaffoni, R. Peverall, and G. A. D. Ritchie, *Opt. Lett.* **39**, 6811 (2014).
21. V. L. Kasyutich and M. W. Sigrist, *Infrared Phys. Technol.* **71**, 179 (2015).
22. V. L. Kasyutich and P. A. Martin, *Opt. Commun.* **284**, 5723 (2011).
23. G. Di Domenico, S. Schilt, and P. Thomann, *Appl. Opt.* **49**, 4801 (2010).
24. L. Tombez, S. Schilt, J. Di Francesco, T. Führer, B. Rein, T. Walther, G. Di Domenico, D. Hofstetter, and P. Thomann, *Appl. Phys. B: Lasers Opt.* **109**, 407 (2012).
25. N. Mukherjee, R. Go, and C. K. N. Patel, *Appl. Phys. Lett.* **92**, 111116 (2008).
26. L. S. Rothman, I. E. Gordon, Y. Babikov, A. Barbe, D. Chris Benner, P. F. Bernath, M. Birk, L. Bizzocchi, V. Boudon, L. R. Brown, A. Campargue, K. Chance, E. A. Cohen, L. H. Coudert, V. M. Devi, B. J. Drouin, A. Fayt, J. M. Flaud, R. R. Gamache, J. J. Harrison, J. M. Hartmann, C. Hill, J. T. Hodges, D. Jacquemart, A. Jolly, J. Lamouroux, R. J. Le Roy, G. Li, D. A. Long, O. M. Lyulin, C. J. Mackie, S. T. Massie, S. Mikhailenko, H. S. P. Müller, O. V. Naumenko, A. V. Nikitin, J. Orphal, V. Perevalov, A. Perrin, E. R. Polovtseva, C. Richard, M. A. H. Smith, E. Starikova, K. Sung, S. Tashkun, J. Tennyson, G. C. Toon, V. G. Tyuterev, and G. Wagner, *J. Quant. Spectrosc. Radiat. Transf.* **130**, 4 (2013).